Journal of Environmental Health Science and Engineering (2021) 19:837–849
https://doi.org/10.1007/s40201-021-00651-8

RESEARCH ARTICLE

Photo-catalytic degradation of bisphenol-a from aqueous solutions using GF/Fe-TiO_2-CQD hybrid composite

Ahmad Jonidi Jafari[1,2] · Roshanak Rezaei Kalantary[2] · Ali Esrafili[2] · Mehrdad Moslemzadeh[2]

Received: 27 December 2020 / Accepted: 15 March 2021 / Published online: 26 March 2021

Abstract

In this photocatalytic study, removal of bisphenol-A from aqueous solution was studied using the GF/Fe-TiO_2-CQD composite. Due to its health and environmental effects, this compound should be disposed of sources that are mainly industrial wastewater. The phis-chemical properties of the composite were determined by traditional analyzes of EF-SEM, EDX, BET, XRD, FTIR and DRS. In this study, different ratios of CQD in the composite (1.5, 4.5 and 7.5 wt%), pH, and bisphenol-A concentration as variable parameters were investigated. All analyzes, EF-SEM, EDX, BET, XRD, FTIR, show that the GF/Fe-TiO_2-CQD composite is well coated on glass fibers (GF) and all the elements in the catalyst are present. On the other hand, DRS analysis showed that CQD reduces the band gap of Fe-TiO_2 from 2.96 eV to 2.91 eV, it was 3.10 eV for TiO_2. Among different catalysts, GF/Fe-TiO_2-$CQD_{4.5wt\%}$ has the best performance. The results showed that for GF/Fe-TiO_2-$CQD_{4.5wt\%}$, optimum for the process was at pH = 6 in low concentration of bisphenol-A. The first order model for the photocatalytic degradation process were well studied. In addition, GF/Fe-TiO_2-$CQD_{4.5wt\%}$ showed that it can be used many times with a minimal reduction in performance. As a result, the GF/Fe-TiO_2-$CQD_{4.5wt\%}$ composite can successfully remove bisphenol-A form in synthetic aqueous solution. However, it is necessary to further studies to applied that for real water source in water and wastewater treatment plants.

Keywords Photo-catalytic · Bisphenol-a (BPA) · Glass Fiber, Fe-TiO_2, carbon quantum dot

Introduction

Bisphenol-A (BPA) is classified in the midst of EDCs since it displays estrogenic activity. Bisphenol-A is a monomer of polycarbonate plastics, which is one of the highest volume chemicals produced worldwide [1, 2]. In the water resources bisphenol-A is known as a threat for the emission health and ecosystems through the food chain. It is a well-known compound which can disturb the endocrine system, which leads to impaired reproduction, obesity, neurological disease, and cancers [3, 4]. The lowest observed affect level for bisphenol-A was determined as 50 μg kg^{-1} body weight day^{-1} by the USEPA, and adapted by the FDA [5]. High bisphenol-A concentrations of 0.0013, 0.056, 0.37, and 17.2 mg L^{-1} were detected in tap water, surface water, effluents from a wastewater plant, and landfill leachate, respectively. The bisphenol-A is difficult to biodegrade and to bio-accumulate so it is persisted in environment. Bisphenol-A is a durable chemical and its natural degradation is slow so that it takes more than 90 years, therefore effective techniques to remove and/or degrade bisphenol-A in the environment are desired [6, 7]. In recent years, some researchers have studied the removal of bisphenol-A using sorption-based processes such as natural adsorbents [8–10] and MOFs [11–13], catalytic processes [14–16], and photocatalytic processes under UV and UV-visible radiation [3, 17–19]. Among these, photocatalytic processes, which is one of the AOP processes, due to their greater environmental compatibility and low cost in environmental treatment, especially in the removal of low-concentration contaminants have been used [3].

Titanium dioxide (TiO_2) is known as one of the most successful semiconductors in the industry due to its very low toxicity, high chemical stability (especially against light corrosion) and photocatalytic applications [20]. In the photocatalytic removal of organic pollutants by TiO_2, UV radiation on

✉ Mehrdad Moslemzadeh
mehrdad.moslemzadh@gmail.com

[1] Research Center for Environmental Health Technology, Iran University of Medical Sciences, Tehran 1449614535, Iran

[2] Department of Environmental Health Engineering, School of Public Health, Iran University of Medical Sciences, Tehran 1449614535, Iran

the surface of TiO_2 leads to the production of electron-holes (e^-/h^+) pairs. The large gap band TiO_2 (3–3.2 ev) limits its photocatalytic activity under visible light radiation. The rapid recombination of the e^-/h^+ pairs produced and the slow transfer of excited electrons is also a major problem of intrinsic semiconductors. On the other hand, very low surface area of TiO_2 leads to narrow absorption of visible light irradiation in the range of 400–760 nm [21, 22]. Several methods have been proposed by researchers to solve the above problems, such as doping of metallic and non-metallic elements [21, 22], sensitization of dye [23], and banding with narrow-band gap semiconductors [24]. Iman et al. have reported that coating TiO_2 on a surface can increase its specific surface area and increase the absorption of UV visible light [25]. Fe^{3+} is considered as a suitable alternative due to its ionic radius similar to Ti^{4+} (Fe^{3+} = 78.5 pm, Ti^{4+} = 74.5 pm), which can be easily replaced in the TiO_2 crystal lattice. In addition, proximity of the redox potential (energy differential) of Fe^{2+}/Fe^{3+} and Ti^{3+}/Ti^{4+} with each other leads to increased light absorption by TiO_2 in the visible region. Due to its availability as well as the above-mentioned properties, Fe was selected as a dopant agent in this study [26]. Fe^{3+} with a gap band energy of 2.2 eV causes a sharp decrease in the TiO_2 gap band from 3 to 3.2 eV to 1.8–2 eV. Fe^{3+} can also act as an electron carrier in the TiO_2 network. It should be noted that high dopant concentrations usually lead to rapid recombination of e^-/h^+ pairs and thermal instability [27].

Recently, carbon quantum dots (CQDs) have been introduced as new types of carbon nanomaterials with sizes below 10 nm. Their characteristics (CQD) include high water solubility, good biological compatibility, low toxicity, and tunable photoluminescence [28]. CQDs have a high ability to transmit excited electrons under light radiation as well as improve the efficiency of e^-/h^+ pairs production. The photoluminescence emission of CQDs is mainly at 430–550 nm. Due to these properties, CQDs have been successfully used for photocatalytic applications to improve the photo-catalytic activity of semiconductors by reducing the recombination of e^-/h^+ pairs and expanding light-sensitive regions. Physical mechanisms such as centrifugation and filtration and the catalysts synthesized with Fe as the core to obtain a magnetic particle, or deposed on substrates such as GAC [22, 29], glass fiber (GF) [25, 30], membrane [31, 32] are the most common methods for recycling catalysts used for water purification.

In the magnetic composite, some of the semiconductor (TiO_2) is deprived of access to light radiation [25]. GF as an amorphous substrate can increase the specific surface area of the photocatalyst when used as a base. Compared to other substrates, GF has some unique properties such as high surface area and flexibility. Some researchers have reported that GF as a preservative for Fe-TiO_2 increases its photocatalytic efficiency for the decomposition of organic matter in aqueous solution [33, 34]. Given the properties mentioned for CQDs and GF, the aim of our study was to fabricate a TiO_2-Fe-CQD composite fixed on glass fibers to degradation of bisphenol-A in aqueous solution under UV-visible light.

The influence of parameters including different percentage of CQD on the fabricated catalyst structure, pH, and initial concentration of bisphenol-A on the efficiency of the bisphenol-A removal process was studied. The properties of the prepared catalysts, adsorption kinetics, pH_{ZPC}, catalyst stability, reaction kinetic study as well as identification of active species were studied. In the following sections, the Fe-TiO_2-CQD fixed on GF is called GF/Fe-TiO_2-CQD for short.

Materials and methods

Experimental

Materials

All of the chemical reagents used in this study were commercial and were used without further refining. Bisphenol-A (98%), titanium tetraisopropoxide (TnBT(Ti $[O(CH_2)_3CH_3]_4$)), $Fe(NO_3)_3{\cdot}9H_2O$ (98%), ascorbic acid, Na_2-EDTA, $AgNO_3$, and sodium azide was made in Merck, Germany. Also, material of HNO_3%, HCl, NaOH, acetonitrile (99%), and ethanol (99.9%) were from Aldrich, USA. GF texture purchased from Shimie afsoon, Tehran, Iran.

Preparation of CQD

CQD was prepared using hydrothermal method based on reference [35]. First, 3 g of citric acid and 1 g of urea were dissolved in 10 ml of distilled water and then heated at 180 °C for 5 h. The suspension was then centrifuged at 10,000 rpm for 30 min to separate larger particles. Finally, the brown solution obtained was kept dry and dark place for further use.

Preparation of GF/Fe-TiO_2-CQD composite

The GF/Fe-TiO_2-CQD composite was prepared by a sol-gel method in two steps.

First step is fabricating GF/Fe-TiO_2, using a sol-gel procedure followed by a dip-coating process adopted reference [33]. In brief, 17 mL of TnBT, 0.5 mL of nitric acid, and 1.5 mL of deionized water were added sequentially to 136 mL of ethanol. This was followed by the addition of 0.1 g of iron (III) nitrate (Fe $(NO_3)_3$ to the solution, resulting in Fe-TiO_2 fabricates. A piece of GF texture (6 × 4 cm) was subsequently dipped into the mixture for 30 min and then pulled out slowly at a rate of 1 cm min^{-1}, and dried an ambient

followed by drying in an oven at 105 °C for 24 h. This was done for three times for high loading.

In the next step, the prepared CQD was coated on GF/Fe-TiO_2. For this purpose, different amounts of CQD solution (1.5, 4.5, and 7.5%wt) were added to 20 ml of ethanol and dispersed by ultrasonics. Then, the GF/Fe-TiO_2 produced in the previous step was immobilized in ethanol solution containing CQD for 30 min. The fibers were then gently removed at a rate of 1 C/min and dried at room temperature, followed by drying in an oven at 105 °C overnight. This was done three times to load more. Finally, the GF/Fe-TiO_2-CQD composite was calcined in an electric furnace at 300 °C in a rate of 2 °C min^{-1} under Nitrogen atmosphere for 3 h.

Characterization

The chemical and physical properties of the prepared catalysts were determined by the following analyzes. The morphology of the catalysts was determined using a field emission scanning electron microscope (FE-SEM, Hitachi S-4800 Japan) with an accelerating voltage of 15.0 kV. The purity and composition of the samples were investigated by FE-SEM equipped with energy dispersion generated by X-ray spectroscopy (EDX). The surface properties and pores of catalysts, Brunauer-Emmett-Teller (BET), were determined by an N_2 adsorption tool (ASAP 2020 μm). Data caused by a Thermofisher Nicolet 6700 spectrometer (Thermofisher, USA) was recorded as FT-IR spectra in the range of from 4000 to 400 cm^{-1}. X-ray diffraction (XRD) patterns of the catalysts were studied using the Rigaku Dmax-RB (Tokyo, Japan) diffractometer. Reflection spectroscopy (DRS) analysis was performed using a Hitachi U-3010 UV-vis (UV-vis) spectrophotometer (Tokyo, Japan).

Photo-catalytic experiments and analysis

Photocatalytic degradation of bisphenol-A was performed in a simple glass chamber (diameter = 50 mm, height = 100 mm). A 55 W xenon lamp with a radiation intensity of 75 mW cm^{-2} and a maximum light output of 472 nm was used as the UV-visible light source above (3 cm) the glass. A piece of GF/Fe-TiO_2-$CQD_{4.5\%wt}$ was fixed inside the glass chamber. Aqueous solution of bisphenol-A was poured into this glass chamber and mixed using a magnetic stirrer. The pH of the solution was adjusted to the desired value with a solution of buffer HCl, NaOH (5, 6, 7, 8, and 9) and the pH meter (PHS-25, Hatch, USA) measured the pH values.

The experiments were performed in two stages, first absorption and then photocatalytic process. To determine the contribution of the adsorption process during the degradation of the bisphenol-A, adsorption tests were performed in the first 30 min before the lamp was turned on. The system was then exposed to UV-visible light for various times.

Photocatalytic degradation efficiency of bisphenol-A was calculated by Eq. (1):

$$DE = \frac{C_1 - C_2}{C_1} \times 100 \quad (1)$$

Where C_1 and C_2 is the initial and final concentration of bisphenol-A before and after irradiation into the solution.

Concentrations of bisphenol-A and other agents were determined using high performance liquid chromatography (HPLC) (using Shimadzu 2010HTC instrument) equipped with Perkin-Elmer C18 column. Bisphenol-A was assayed with acetonitrile-water mixture (60:40 *v*/v) as the carrier phase at a flow rate of 1 ml min^{-1} and a UV absorption wavelength of 218 nm. The column temperature was kept at about 45 °C during the analysis. The volume of each sample injected into the device was 20 μl.

Result and discussion

Photo-catalytic characterization

SEM and EDX analysis

FE-SEM analysis was used to investigate the morphology of the samples. Figure 1 shows the data obtained from the FE-SEM analysis for GF/Fe-TiO_2-$CQD_{4.5wt\%}$ (a) and row GF (b). Looking at the image of FE-SEM (a), a thin layer of Fe-TiO_2-CQD is clear on the GF surface, while this catalytic coating was not on the GF surface (b). EDX analysis was used to determine the sample elements. Figure 1 (c, d, and e) shows the data obtained from EDX analysis of GF/Fe-TiO_2-CQD samples with different percentages of CQD (1.5, 4.5, and 7.5 wt%). This analysis showed that CQD was evenly distributed on the particles, in addition, with increasing CQD in the synthesized samples, its concentration increased.

BET study

A review of previous research shows that the surface properties of catalysts have a very significant effect on the efficiency of the photocatalytic process [36]. Therefore, nitrogen adsorption and desorption isotherms were performed to obtain the specific surface area, pore diameter and pore volume of the samples, and the results are presented in Fig.2a and Table 1. According to the results, when Fe-TiO_2 was coated on GF, the average pore diameter increased while the specific surface area and pore volume decreased. Such results have been reported by Imane Benyamina et al. [25]. The specific surface area of Fe-TiO_2 and GF/Fe-TiO_2 samples were 468 and 525.1 m^2/g, respectively (Table 1). The Fe-TiO_2-$CQD_{4.5\%wt}$ composite had lower pore surface and volume than GF/Fe-

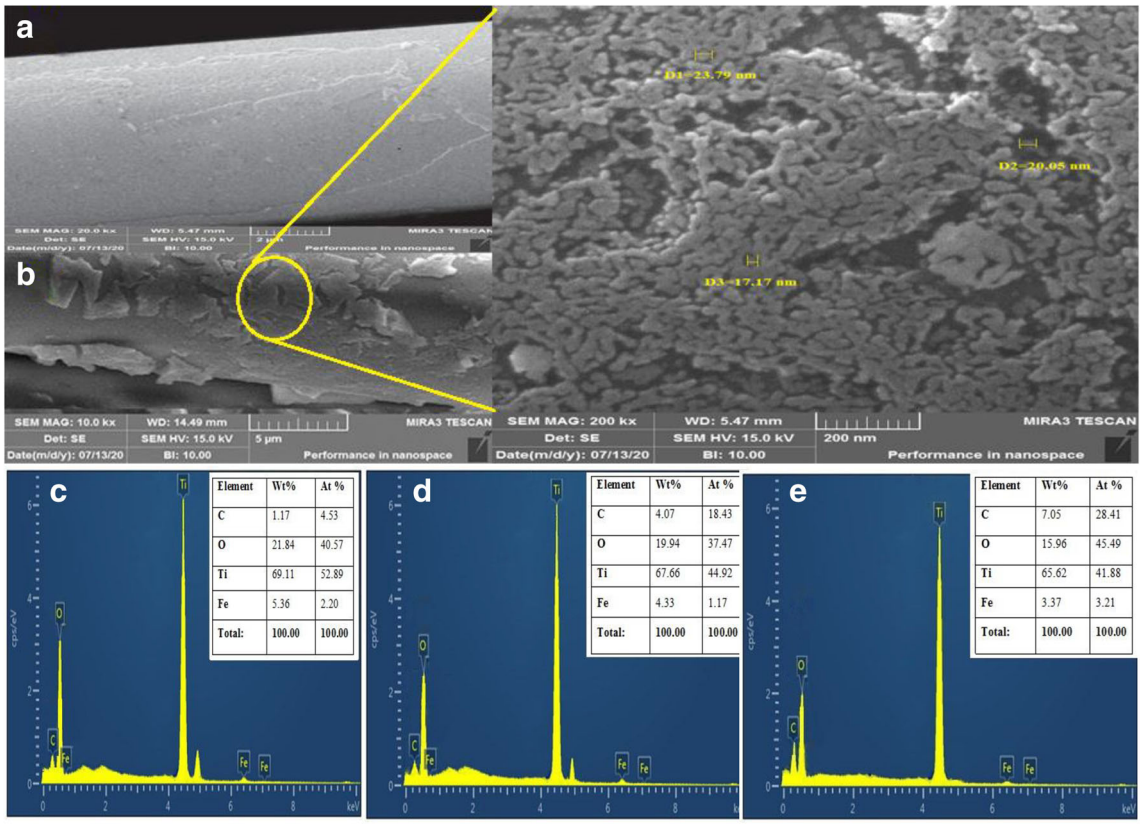

Fig. 1 FE-SEM of GF (**a**) and GF/Fe-TiO_2-$CQD_{4.5wt\%}$ (**b**), EDX of the GF/Fe-TiO_2-CQD (1.5 (**c**), 4.5 (**d**), and 7.5 (**e**) wt%)

TiO_2 while its average pore diameter was higher than GF/Fe-TiO_2 (Table 1). GF/Fe-TiO_2 had a specific surface area of 525.1 m^2/g. Addition of CQD to GF/Fe-TiO_2 reduced its specific surface area (538.5 m_2/g). This decrease occurred at CQD's percentages above 4.5%wt and resulted in a slight decrease in the degradation efficiency of bisphenol-A.

FT-IR spectra

The FTIR spectra of the synthesized samples are shown in Fig. 2b. The order of the spectra in this FTIR diagram is CQD (a), Nano Fe_2O_3 (b), TiO_2 (c) and Fe-TiO_2-CQD (d). FTIR results show four main absorption peaks located in the regions 475–573, 1078–1109, 1619–1937, 3025–3515 cm^{-1}. In the range of 475–573 cm^{-1}, there is an absorption spectrum that was related to the stretching vibration of Fe-O and Ti–O [36]. The adsorption in the region of 1619–1637 cm^{-1} was related to the bending vibrations of the hydroxyl present on the surface of TiO_2 and TiO_2-Fe-CQD. This hydroxyl can be caused by partial moisture in the photocatalyst [37]. In the CQD spectrum (Fig. 2b(a)),there are the adsorptions in the regions of 3025 and 3515 cm^{-1}, 1390 cm^{-1}, and 1173 cm^{-1} which are related to –N-H stretch, $COCH_2$-bending, and C-N bond, respectively [38]. A short and wide adsorption at 3452 cm^{-1} was observed which is related to Ti-OH and Fe-OH and caused by water molecules that are attached by weak hydrogen bonds [6]. In general, FTIR results confirm the presence of metal oxides and surface functional groups related to the presence of CQD.

XRD analysis Figure 3a shows XRD pattern of the samples included pure TiO_2 and Fe-TiO_2-$CQD_{4.5wt\%}$ synthesized by sol-gel method. From the analysis, the peak of pure TiO_2 is matched with pattern no. JCPDS 00–021-1272, which corresponded to anatase phase [39]. This peak is also detected in with another sample (Fe-TiO_2-CQD). From this analysis, the peak of the pure TiO_2 and Fe-TiO_2-CQD were detected at diffraction angles of 22.35°, 37.90°, 47.90°, 53.96°, 62.66°

Table 1 The specific surface area, pore diameter, and pore volume of the samples

Photocatalysts	BET surface area (m^2 g^{-1})	Pore Volume (cm^3 g^{-1})	Pore Diameter in nm
GF/Fe-TiO_2-$CQD_{4.5wt\%}$	538.5	0.560	4.32
GF/Fe-TiO_2	552.1	0.747	3.57
Fe-TiO_2	468.0	0.418	4.49

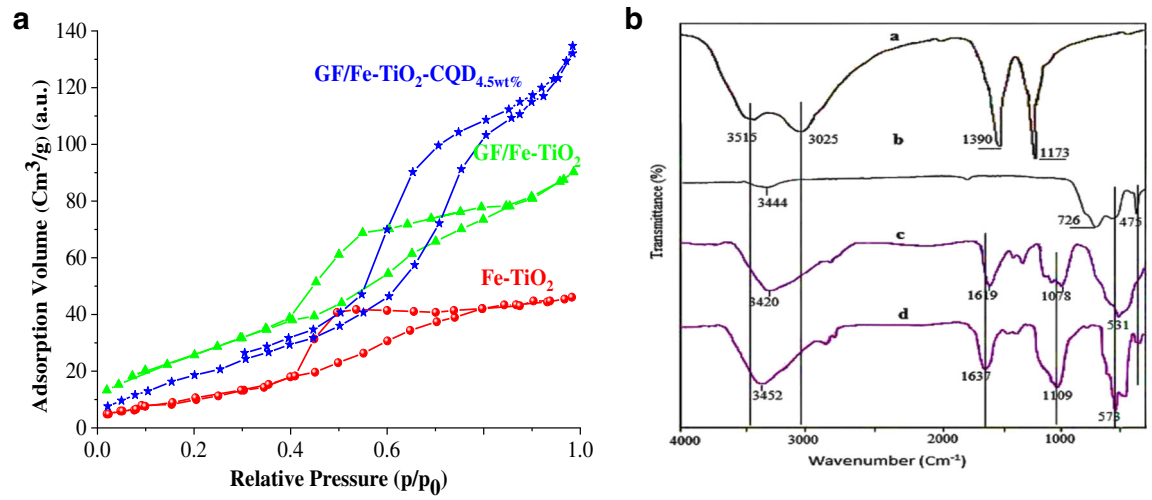

Fig. 2 (**a**) The N_2 adsorption–desorption isotherms of the samples, (**b**) the FTIR spectrum of the samples; (**a**) CQD, (**b**) Fe_2O_3, (TiO_2) and (Fe-TiO_2-$CQD_{4.5wt\ \%}$)

which corresponded to (101), (004), (200), (105), (211) and (204) plane, respectively. In addition, no peak associated with Fe was observed for pattern of Fe-TiO_2-CQD. This indicates the formation of iron-titanium solid solution where the Fe was successfully incorporated into TiO_2 lattice structure due to the similarity of ionic radius size between Ti^{4+} (0.68 A°) and Fe^{3+} (0.64 A°) mentioned in the introduction section [40–42]. Also, as can be seen in EDX analysis data (Fig. 1b), amount of Fe is very low. Therefore, all of these events led to disappearing of Fe in XRD pattern of Fe-TiO_2-CQD.

UV-Vis DRS and band gap determination

UV–visible diffuse reflectance spectra of CQD, un-doped TiO_2, Fe-TiO_2 and Fe-TiO_2-$CQD_{1.5,\ 4.5\ and\ 7.5\ wt\%}$ samples are shown in Fig. 3b. Fe-TiO_2 shows improved absorptions in the range of 380 to 500 nm. The spectrum for the undoped TiO_2 has a sharp absorption edge at 365 nm. However, the absorption threshold of Fe-TiO_2 shifted in the visible region of the spectrum. The enhanced visible light absorptions may be explained by the charge-transfer transition between the d-electrons of the Fe-dopant and the conduction band of TiO_2 [43]. Fe-TiO_2-CQD shows high enhanced absorptions after 400 nm with increasing CQD content. The enhanced visible light absorptions may be explained by the charge-transfer transition between the conduction band of TiO_2 and CQD [44]. Also, CQD has strong absorption in all over of spectra from 300 to 700 nm (Fig. 3b). The absorption measurement of Fe-TiO_2-CQD 1.5, 4.5 and 7.5 wt% showed absorption at 400, 418 and 425 nm, respectively, whereas TiO_2 and Fe-doped TiO_2 absorption at 375 and 390 nm, respectively.

The band gap energy was calculated using Kubelka-Munk principles as shown in the Eq. (2) [44]:

$$E_{g=}\frac{1,240}{\lambda} \tag{2}$$

The band gap energy for un-doped TiO_2, Fe-TiO_2 and Fe-TiO_2-CQD 1.5, 4.5 and 7.5 wt% were 3.10, 2.96 and 2.91, respectively. All these samples showed a reduction in band gap energy as a result of surface modification of TiO_2.

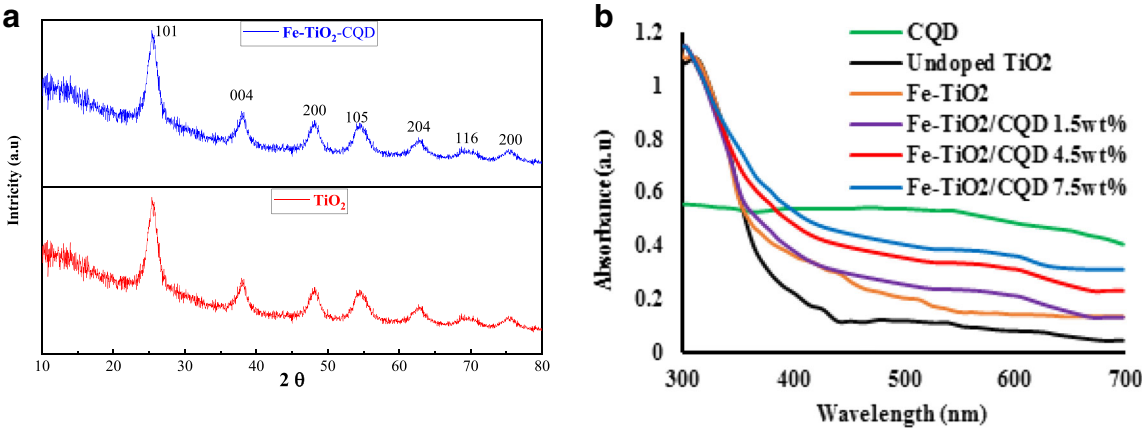

Fig. 3 The XRD (**a**), UV-vis diffuse reflectance spectra (DRS) (**b**) of the Fe-TiO_2-CQD

Performance of the prepared materials

In a photocatalytic degradation process, several factors can work together to remove contaminants. In our study, the degradation of bisphenol-A was examined separately by visible light and GF lonely, GF TiO_2, GF/Fe-TiO_2, and GF / Fe-TiO2-$CQD_{4.5\%wt}$ under visible and UV light. In these studies, the time for dark and light conditions was 30 min, the concentration of bisphenol-A was 20 mg l^{-1}, which was done at normal pH (6.5) and the results of the experiments are shown in Fig. 4. As can be seen, visible light with was only able to remove 6% of bisphenol-A in 30 min of dark condition. This decrease occurred due to the adsorption of bisphenol-A on GF and photolysis by visible light [45]. The results show that the removal efficiencies for GF/TiO_2 and GF/Fe-TiO_2 under visible light were 41% and 81%, respectively. As discussed in the catalytic photo description section, doping TiO_2 with Fe can improve the performance of bisphenol-A photo-degradation. The main photocatalyst in this work was GF/Fe-TiO_2-$CQD_{4.5wt\%}$ which was studied separately with visible light and ultraviolet light for the degradation of bisphenol A. Figure 4 shows that in the presence of visible light and ultraviolet UV light, GF/Fe-TiO_2-$CQD_{4.5wt\%}$ was able to remove nearly 100% of bisphenol-A.

Photo-catalytic performance

Kinetic of adsorption

The first step for a successful photocatalytic process is to direct the pollutant to the surface of the catalyst, which occurs in the adsorption operation [25]. Therefore, the adsorption kinetics of the process were investigated when the concentration of bisphenol-A, and pH were 50 mg L^{-1} and normal (6.5),

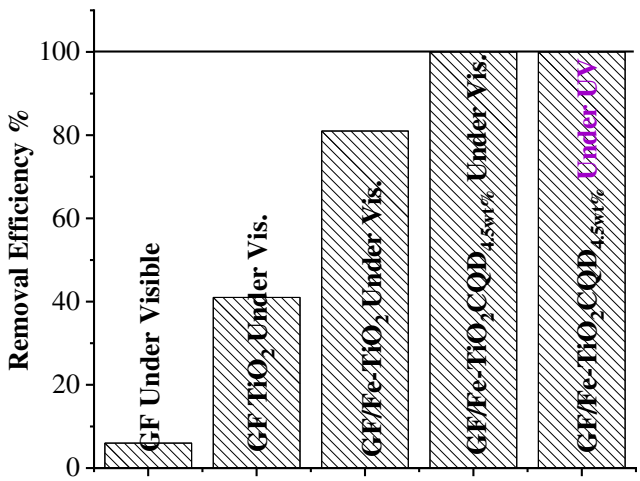

Fig. 4 Comparative study between the prepared materials

respectively. The maximum adsorption (Qmax) was calculated in equilibrium with Eq.

$$Q_{max} = \frac{(C_c - C_e)V}{M} \quad (3)$$

Where C_0 is the initial concentration of bisphenol-A in the solution (mg L^{-1}), C_e is the equilibrium concentration (mg L^{-1}), M is the mass of the GF/Fe-TiO_2-$CQD_{4.5wt\ \%}$ (g), and V is the volume of solution (L). The results are published in Fig. 5(a). According to Fig. 5(a), the adsorption system for GF/Fe-TiO_2-$CQD_{4.5\%wt}$ achieved equilibrium in 30 min and the Q_{max} for bisphenol-A at this time was 8 mg g^{-1}. According to other studies, this adsorption capacity was optimal and could be an advantage for this process [6, 46].

Effect of different amount of the CQD

In order to investigate effects of different amount of CQD on the fabrication of the prepared catalysts on the efficiency of the photocatalytic process, experiments under conditions that concentration of bisphenol-A and pH were 20 mg L^{-1} and normal (6.5), respectively. For this experiment, three types of GF/Fe-TiO_2-CQD composites were used, which had percentages 1.5, 4.5, and 7.5 wt% of CQD, and the results of bisphenol-A photo degradation under visible light are presented in Fig. 5(b). The results showed higher performance for GF/Fe-TiO_2-$CQD_{4.5wt\ \%}$ than the other two composites. As the percentage of CQD in the catalysts increased to 4.5 wt%, the degradation efficiency increased, while as the increase continued to 7.5 wt%, the degradation efficiency decreased. Therefore, at a weight percentage of 4.5 wt% for CQD, the efficiency is at its highest. The reason for this phenomenon is the attraction lighter on this percentage of CQD and then the efficiency is reduced due to darkness and light reflection by CQD [19]. In addition, as described in the BET analysis section, the presence of CQD in the catalyst structure covers part of its surface area and leads to a decrease in specific surface area, which occurs at higher CQD levels. Therefore, the surface of the catalyst and the contact of its active substance (TiO_2) with light is reduced [19, 46].

Effect of pH

The pH is often a serious factor in the photo-degradation removal of contaminants from aqueous solution due to its capability to affect the surface charge of the heterogenic photocatalyst and existing form of the contaminants [47]. It is believed pH may impact the photo-catalytic activity of GF/Fe-TiO_2-$CQD_{4.5wt\%}$ therefore that was surveyed in concentration of bisphenol-A 20 mg L^{-1} and deferent pH values (5, 6, 7, 8, and 9). Figure 5(c) shows the effect of initial pH on the photo-

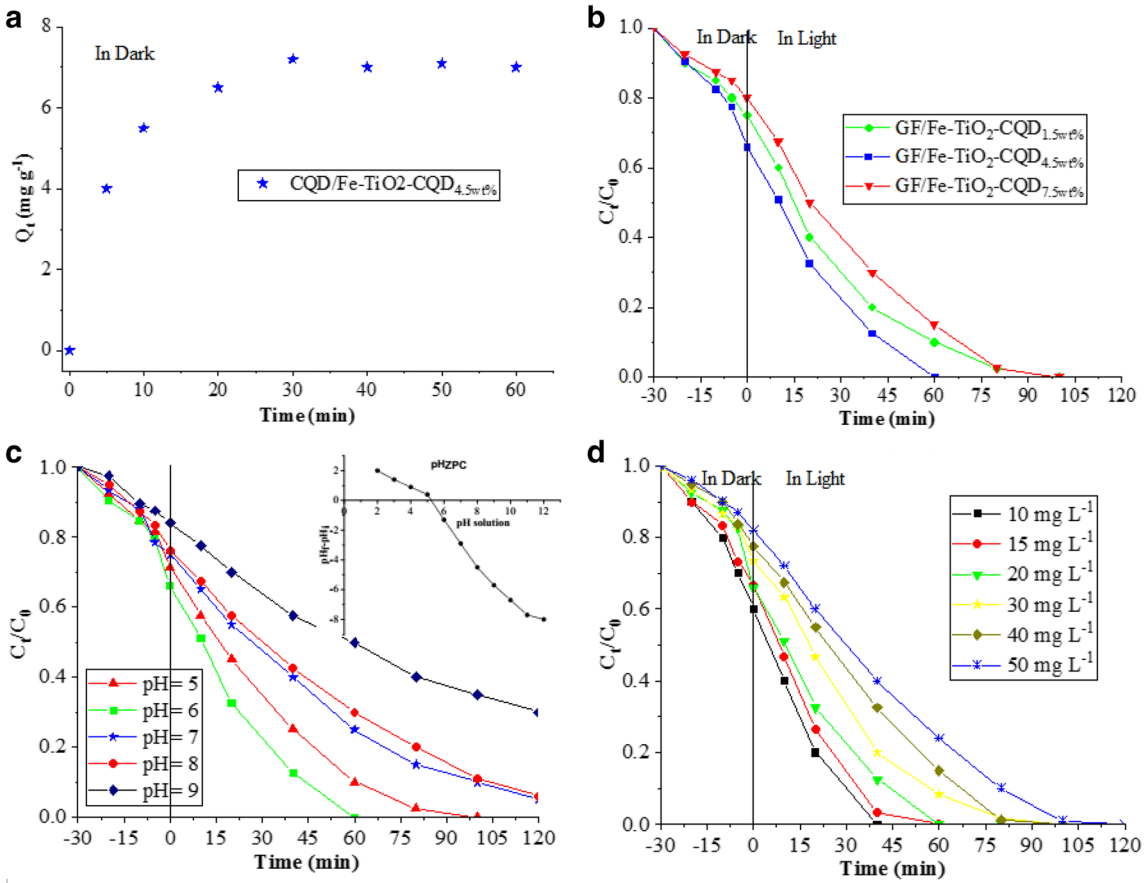

Fig. 5 Effect of parameters on the efficiency of the process; adsorption kinetic (**a**), and different amount of the CQD (**b**), pH (**c**), and concentration of bisphenol A (**d**)

degradation efficiency of bisphenol-A onto the GF/Fe-TiO_2-$CQD_{4.5wt\%}$ under illumination. Result showed that 100% of bisphenol-A was removed onto the GF/Fe-TiO_2-$CQD_{4.5wt\%}$ at pH = 6 after 60 min of illumination. Also, the photo-degradation efficiency of bisphenol-A reached to 100% at pH 5 in 100 min. However, the photo-degradation efficiency decreased when the pH up to 9, where only 50% of the initial bisphenol-A removed after 60 min. These results were mainly related to the pH_{ZPC} of GF/Fe-TiO_2-$CQD_{4.5wt\%}$ and pK_a of bisphenol-A. As mentioned at the adsorption kinetic section, the rate of reaction depends on the adsorption at the solid-liquid interface. First de-protonation of bisphenol-A triggers at around pH = 8 and the other one starts at around pH 9, so $pK_{a1}$and pK_{a2} of bisphenol-A are 8 and 9, respectively [18]. Hence, when the solution pH is higher than 8, bisphenol-A becomes negatively charged. As shown in Fig. 5(c), the pH_{PZC} of GF/Fe-TiO_2-$CQD_{4.5wt\%}$, which determined as our previous work method, is 5.3, thus it is negatively charged at higher than this point. In result, this leads to the electrostatic adsorption between the GF/Fe-TiO_2-$CQD_{4.5wt\%}$ and bisphenol-A molecules. Now, adsorbed the molecules onto the photo-catalyst react with active regent discussed in further at the identification of active species section. In spite to some results declaring opposite role regarding pH effect [1, 18, 48], there are many studies that report similar behave abut effect of pH on the photo-degradation of bisphenol-A [2, 17, 18, 49].

Effect of concentration

The effect of initial concentration of bisphenol-A on the process of photocatalytic degradation was performed at pH = 6 and different concentrations of bisphenol-A (10, 20, 30, 40 and 50 mg L^{-1}) and the results are reported in Fig. 5(d). It can be deduced from Fig. 5(d) that increasing the concentration had a negative effect on the removal efficiency, as increasing the concentration of bisphenol-A led to a decrease in the inverse degradation efficiency of bisphenol-A. At a constant GF/Fe-TiO_2-$CQD_{4.5wt\%}$ mass, efficiency will be dictated by the catalyst active sites to substrate molecules ratio [50]. This phenomenon may be related to the reduction in the availability of bisphenol-A to active sites, which leads to the initiation of a competitive adsorption between bisphenol-A and the by-products of the reaction on the catalyst surface, thus reduces the volume of oxidizing species attacking bisphenol A [25].

Table 2 Calculated parameter values of the pseudo-first order and pseudo-second order

C_i (mg L^{-1})	K_1 (min^{-1})	R^2	K_2 (mg L^{-1}.min)	R^2
10	0.049	0.9994	0.0104	0.7945
15	0.0458	0.9839	0.0075	0.9423
20	0.0426	0.9887	0.0084	0.9196
30	0.0375	0.9825	0.0058	0.877
40	0.0275	0.9738	0.0022	0.8763
50	0.0255	0.9634	0.002	0.8001

Kinetic of reaction

To study the mechanism of photo-degradation kinetics of process and the degradation behavior of the process was analyzed using the kinetic models. In this study, the applicability of the pseudo-first and pseudo-second order kinetics were tested for the photo-degradation kinetics of bisphenol-A on the GF/Fe-TiO_2-$CQD_{4.5wt\%}$. Linear form of them is shown via Eq. (4) and (5) [51].

$$lnC_t = lnC_0 - k_1 t \tag{4}$$

$$\frac{1}{C_t} = \frac{1}{C_2} + k_2 t \tag{5}$$

Where, C_0, and C_t are bisphenol-A concentrations at times 0 and t (min), respectively. k_1 (min^{-1}) and k_2 (mg L^{-1}. min) are the first and second order reaction coefficients, respectively.

The plots of LnC_t and $1/C_t$ versus reaction time are depicted in Fig. 6(a,b) for GF/Fe-TiO_2-$CQD_{4.5wt\%}$ and their parameter values were prepared in Table 2. In view of this results, the coefficient of determination (R^2) in all reactions for pseudo-first order was higher than pseudo-second order model, which proved that the experimental kinetic data fit well with the pseudo-first order model. Additionally, rate constants reduced with increased initial concentration of bisphenol-A. Finally, it be concluded that the highest photo-catalytic activity for the bisphenol-A by GF/Fe-TiO_2-$CQD_{4.5wt\%}$ occurred in low initial concentration.

Isotherm experiments

The adsorption isotherm was used to investigate distribution of bisphenol-A molecules onto the GF/Fe-TiO_2-$CQD_{4.5\%wt}$ in equilibrium. The relationship between the concentration of GF/Fe-TiO_2-$CQD_{4.5\%wt}$ in solution and removed bisphenol-A was determined using the Langmuir isotherm and Freundlich [52]:

The Langmuir isotherm model describes monolayer distribution of solute molecules onto the adsorbent surface. The linear form of Langmuir model is expressed via Eq. (6)

$$\frac{C_e}{q_e} = \frac{1}{K_L q_m} + \frac{C_e}{q_m} \tag{6}$$

The Langmuir constants (q_m, K_L and C_e) related to maximum adsorption capacity (mg g^{-1}), the energy of adsorption (L mg^{-1}) and equilibrium concentration of dye in solution (L mg^{-1}), respectively, are calculated from the plot C_e/q_e versus C_e.

Freundlich isotherm model evaluates the multilayer absorption of adsorbate on the absorbent surface. It also assumes that adsorption occurs on heterogeneous surfaces, it can be expressed via Eq. (7)

$$lnq_e = lnK_f + \frac{1}{n}(lnC_e) \tag{7}$$

The parameters K_f and n are Freundlich constants are adsorption capacity (mg g^{-1}) and the adsorption intensity of the system determined from the plot of lnq_e versus lnC_e.

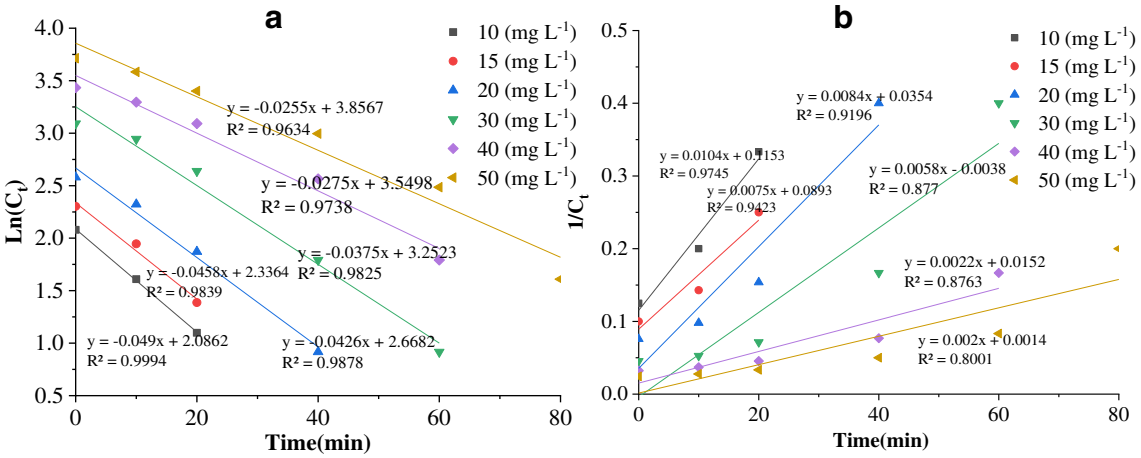

Fig. 6 Study of reaction kinetics; plots of (**a**) pseudo-first and (**b**) pseudo second order models

Table 3 Values of bisphenol-A isotherm parameters

Langmuir isotherm	Parameters	Freundlich isotherm	Parameters
12.75	q_m (mg g^{-1})	1.28	K_F (mg g^{-1})
0.0823	K_L (L mg^{-1})	1.38	N
0.9822	R^2	0.9783	R^2

Figure 7a,b, show Langmuir isotherm for GF/Fe-TiO_2-$CQD_{4.5wt\%}$ and its results are presented in Table. Langmuir isotherm fittings for GF/Fe-TiO_2-$CQD_{4.5wt\%}$ have good coefficient of determination ($R^2 = 0.9822$), also, Langmuir constants, q_m and K_L are obtained 12.75 mg g^{-1} and 0.0823, respectively. Freundlich constants, K_f and n are calculated from the plot of $\ln q_e$ versus $\ln C_e$ not provided here which are 1.28 mg g^{-1} and 1.38, respectively, also coefficient of determination (R^2) for Freundlich isotherm is 0.9783 (Table 3). The value of n is larger than 1 which indicates a favorable adsorption system and a physical process. From the Table 3, it can be concluded that the adsorption of bisphenol-A onto the GF/Fe-TiO_2-$CQD_{4.5wt\%}$ has a better coefficient of determination (R^2) of 0.9823 for Langmuir isotherm than Freundlich isotherm indicating the Langmuir isotherm suitability.

Characterization of active species

Information about the active species contributed in the reaction is very important in view of practical application of photo-catalysts. The most active species in heterogeneous photocatalytic reactions are superoxide radicals ($O_2^{\circ-}$), singlet molecular oxygen ($^1O_2$), hydroxyl radical (HO°), and photogenerated hole (h^+) [25, 53]. Figure 8 shows the effect of the inhibitor on the photo-catalytic efficiency of bisphenol-A photo-degradation with GF/Fe-TiO_2-$CQD_{4.5wt\%}$ as photo-catalyst. A total bisphenol-A degradation efficiency was obtained

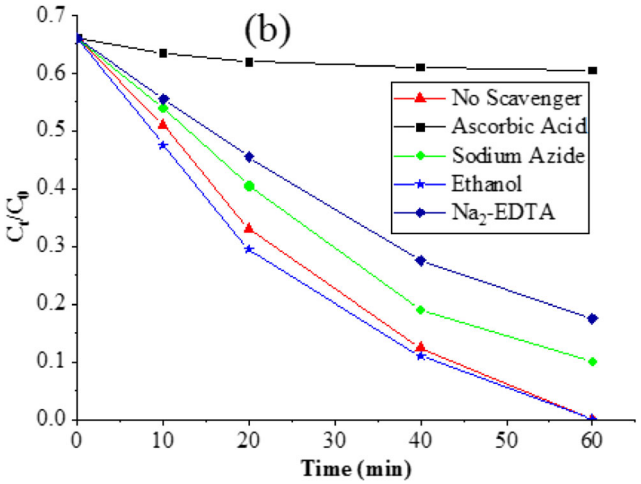

Fig. 8 Identification of active species on the photocatalytic process

after 60 min irradiation under visible light with ethanol or without any scavenger. Only 11% of photo-degradation was obtained over the same time when ascorbic acid was added. However, the addition of sodium azide and Na_2-EDTA produced a slight decrease in the discoloration rate 90% and 83%, respectively. As shown, this result indicates that the species responsible for the bisphenol-A photo-degradation is the superoxide radicals ($O_2^{\circ-}$) with a slight contribution of the photo generated e^-/h^+ pair (the % bisphenol-A removal decreased as compared with the no scavenger). It appears that the(HO°) radicals had no contribution in the mechanism. Data of the past studies confirm significant contribution of ($O_2^{\circ-}$) degradation of organic compounds [54, 55]. Also, the ($^1O_2$) and h^+ are as important agents in a number of chemical processes [48, 56, 57]. These are one of the main activated species responsible for degradation of bisphenol-A. The superoxide radicals ($O_2^{\circ-}$), was found to be the primary species contributing to the degradation of bisphenol-A in GF/Fe-TiO_2-$CQD_{4.5wt\%}$, since ascorbic acid was the most significant scavenging agent.

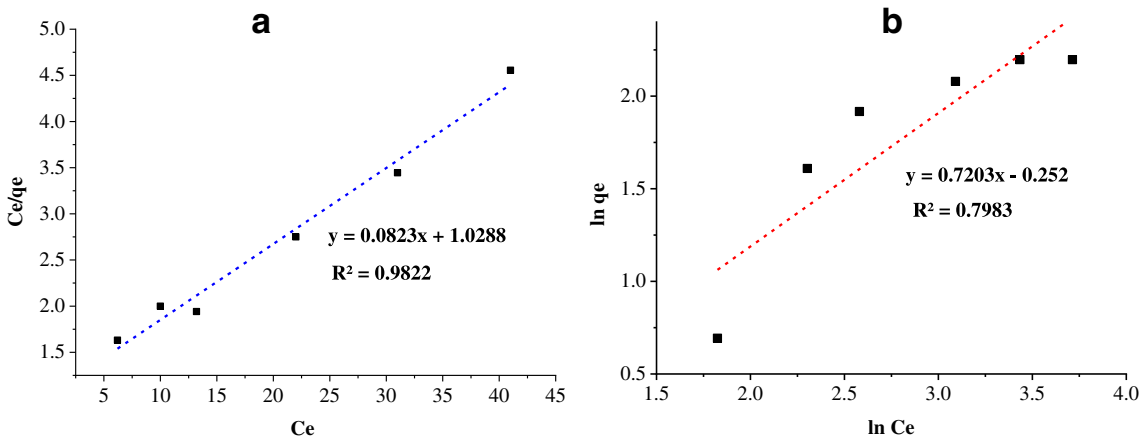

Fig. 7 Adsorption isotherms of bisphenol-A onto GF/Fe-TiO_2-$CQD_{4.5wt\%}$ (**a**) Langmuir and (**b**) Freundlich

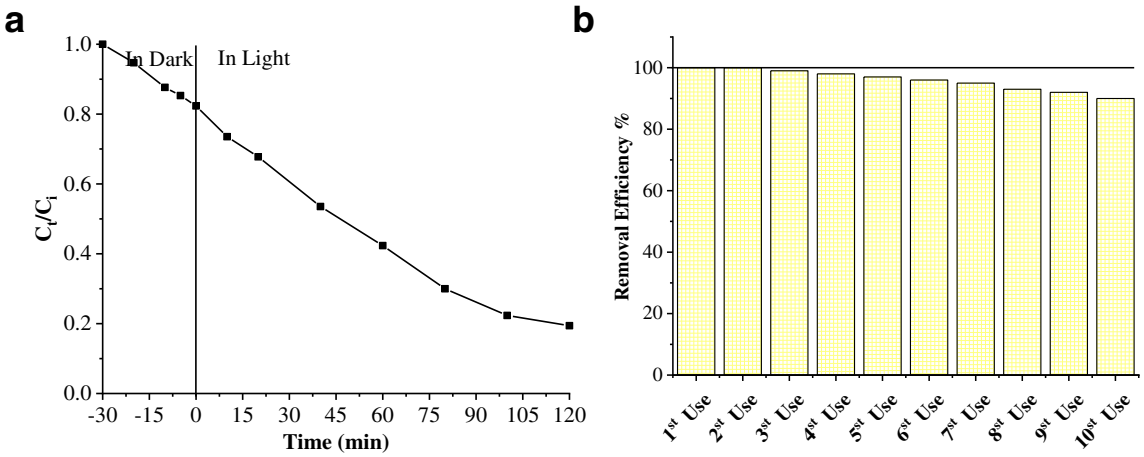

Fig. 9 The performance on real waste water (**a**), and reusability and stability of GF/Fe-TiO_2-$CQD_{4.5wt\%}$ (**b**)

The performance on real wastewater

In our study GF/Fe-TiO_2-$CQD_{4.5wt\%}$ was used to real wastewater as a post treatment. To do this the sample, gathered from effluent of a wastewater treatment plant in south of Tehran, filtered and centrifuged to remove its suspended solids. Then, its chemical contents were determined. In forward, concentration of bisphenol-A in the natural sample was set at 20 mg L^{-1}. At natural pH (6.8) and concentration of bisphenol-A 20 mg L^{-1}, photo-degradation process was conducted, which results show in Fig. 7a. As the result, the removal efficiency of bisphenol-A extremely reduced, so that approximately more than 18% of the pollutant remind in the solution. It accrued mainly because of increased turbidity esteem from colloidal particles and other organic consumed active species [47, 56, 58]. Also, poisoning of catalyst in result of adsorption of contaminants onto the catalyst surface may shield catalyst against the irradiation.

Photo-catalyst reusability and stability study

The stability of the GF/Fe-TiO_2-$CQD_{4.5wt\%}$ photo-catalyst was verified by its photo-catalytic efficiency as a function of reuse number on bisphenol-A photo-degradation in the same conditions during 120 min for each use. As can be seen in Fig. 9b, for tow first runs achieved the same photo-degradation efficiency, whereas from the third run use, the composite begins to lose slightly its effectiveness. Actually, the photo-degradation efficiency 90% was obtained in 10st run. This stability is promising in comparison of other studies [15, 18, 48]. These results indicate the GF/Fe-TiO_2-$CQD_{4.5wt\%}$ could use efficiently and with high stability for photo-degradation of bisphenol-A.

Conclusion

Our study investigated photo-catalytic degradation of bisphenol-A from aqueous solutions using hybrid composite of GF/Fe-TiO_2-CQD. From its results can be concluded as follow:

- Addition of CQD to Fe-TiO_2 in an acceptable volume can well improve light adsorption at visible range, which was demonstrated by DRS analysis.
- In low concentration of Fe in the composite fabrication, that replace in the TiO_2 lattice and can not to be seen in the XRD spectrum.
- Optimizing of the effective parameters could prove the results of characterization analysis.
- As expectation, some scavengers could influence on the photocatalytic process.
- The BET results show that supporting Fe-TiO_2 onto the GF enhanced its surface area wile if CQD on the composite was higher than 4.5 wt% its surface area was decreased, thereby can reduce the performance of process.
- GF can be as a promising supporter for the Fe-TiO_2-CQD composite because well fix the composite and has less leaching. These properties have been shown in the EF-SEM and proved by photo-catalyst reusability and stability study.
- It can be concluded that photocatalytic degradation of bisphenol-A fit well pseudo-first order kinetic and its adsorption behavior be better descripted with Langmuir isotherm.

In general, it can be concluded that hybrid composite of GF/Fe-TiO_2-CQD could successfully remove bisphenol-A form synthetic aqueous solution. However, it needs to further study for application that on real water source at water and wastewater treatment plants.

Acknowledgments The present study was adapted from the PhD thesis of Mehrdad Moslemzadeh at Iran University of Medical Sciences.

Availability of data and materials All data generated or analyzed during this study are included in this published article.

Author's contributions Ahmad Jonidi Jafari: Investigation, Writing - original draft Writing – review & editing.
Roshanak Rezaei Kalantary; Ali Esrafili: Writing – review & editing.
Mehrdad Moslemzadeh: Supervision, Writing – review & editing.

Funding The present project was financially funded by grant number 98–4–2-16,676 from Iran University of Medical Sciences.

Declarations

Ethical approval Not applicable.

Consent to participate Not applicable.

Consent to publish Not applicable.

Conflict of interest The authors declare that they have no conflict of interest.

References

1. Vakili M, Mojiri A, Kindaichi T, Cagnetta G, Yuan J, Wang B, et al. Cross-linked chitosan/zeolite as a fixed-bed column for organic micropollutants removal from aqueous solution, optimization with RSM and artificial neural network. J. Environ. Manage. [internet] 2019;250:109434. Available from: https://doi.org/10.1016/j.jenvman.2019.109434, 2019.
2. Hacıosmanoğlu GG, Doğruel T, Genç S, Oner ET, Can ZS. Adsorptive removal of bisphenol a from aqueous solutions using phosphonated Levan. J Hazard Mater. 2019;374:43–9.
3. Zhou Y, Lu J, Liu Q, Chen H, Liu Y, Zhou Y. A novel hollow-sphere cyclodextrin nanoreactor for the enhanced removal of bisphenol a under visible irradiation. J. Hazard. Mater. [internet] 2020;384:121267. Available from: https://doi.org/10.1016/j.jhazmat.2019.121267, 2020.
4. Li X, Zhou M, Jia J, Ma J, Jia Q. Design of a hyper-crosslinked β-cyclodextrin porous polymer for highly efficient removal toward bisphenol a from water. Sep. Purif. Technol. [internet] 2018;195:130–7. Available from: https://doi.org/10.1016/j.seppur.2017.12.007, 2018.
5. Chen ZH, Liu Z, Hu JQ, Cai QW, Li XY, Wang W, et al. β-Cyclodextrin-modified graphene oxide membranes with large adsorption capacity and high flux for efficient removal of bisphenol a from water. J. Memb. Sci. [internet] 2020;595:117510. Available from: https://doi.org/10.1016/j.memsci.2019.117510, 2020.
6. Fang Z, Hu Y, Cheng J, Chen Y. Continuous removal of trace bisphenol a from water by high efficacy TiO2 nanotube pillared graphene-based macrostructures in a photocatalytically fluidized bed. Chem. Eng. J. [internet] 2019;372:581–9. Available from: https://doi.org/10.1016/j.cej.2019.04.129, 2019.
7. Saroyan HS, Bele S, Giannakoudakis DA, Samanidou VF, Bandosz TJ, Deliyanni EA. Degradation of endocrine disruptor, bisphenol-A, on an mixed oxidation state manganese oxide/modified graphite oxide composite: A role of carbonaceous phase. J. Colloid Interface Sci. [Internet] 2019;539:516–24. Available from: http://www.sciencedirect.com/science/article/pii/S0021979718315297
8. López-Ramón MV, Ocampo-Pérez R, Bautista-Toledo MI, Rivera-Utrilla J, Moreno-Castilla C, Sánchez-Polo M. Removal of bisphenols A and S by adsorption on activated carbon clothes enhanced by the presence of bacteria. Sci. Total Environ. [Internet] 2019;669:767–76. Available from: http://www.sciencedirect.com/science/article/pii/S0048969719311076
9. Choi Y-K, Kan E. Effects of pyrolysis temperature on the physicochemical properties of alfalfa-derived biochar for the adsorption of bisphenol A and sulfamethoxazole in water. Chem Int. 2019;218:741–8 Available from: http://www.sciencedirect.com/science/article/pii/S0045653518322586.
10. Zhou L, Richard C, Ferronato C, Chovelon J-M, Sleiman M. Investigating the performance of biomass-derived biochars for the removal of gaseous ozone, adsorbed nitrate and aqueous bisphenol A. Chem. Eng. J. [Internet] 2018;334:2098–104. Available from: http://www.sciencedirect.com/science/article/pii/S1385894717320673
11. Bhadra BN, Lee JK, Cho CW, Jhung SH. Remarkably efficient adsorbent for the removal of bisphenol a from water: bio-MOF-1-derived porous carbon. Chem Eng J. 2018;343:225–34.
12. Lin Q, Wu Y, Jiang X, Lin F, Liu X, Lu B. Removal of bisphenol A from aqueous solution via host-guest interactions based on beta-cyclodextrin grafted cellulose bead. Int. J. Biol. Macromol. [Internet] 2019;140:1–9. Available from: http://www.sciencedirect.com/science/article/pii/S014181301933329X
13. Luo Z, Chen H, Wu S, Yang C, Cheng J. Enhanced removal of bisphenol a from aqueous solution by aluminum-based MOF/sodium alginate-chitosan composite beads. Chemosphere [internet] 2019;237:124493. Available from: https://doi.org/10.1016/j.chemosphere.2019.124493, 2019.
14. Chen S, Chi M, Yang Z, Gao M, Wang C, Lu X. Carbon dots/Fe3O4 hybrid nanofibers as efficient peroxidase mimics for sensitive detection of H2O2 and ascorbic acid. Inorg Chem Front. 2017;4:1621–7.
15. Li G, Zhang X, Sun J, Zhang A, Liao C. Effective removal of bisphenols from aqueous solution with magnetic hierarchical rattle-like co/Ni-based LDH. J. Hazard. Mater. [internet] 2020;381:120985. Available from: https://doi.org/10.1016/j.jhazmat.2019.120985, 2020.
16. Baran W, Adamek E, Sobczak A, Makowski A. Photocatalytic degradation of sulfa drugs with TiO2, Fe salts and TiO2/FeCl3 in aquatic environment-kinetics and degradation pathway. Appl Catal B Environ. 2009;90:516–25.
17. Xu L, Yang L, Johansson EMJ, Wang Y, Jin P. Photocatalytic activity and mechanism of bisphenol a removal over TiO2−x/rGO nanocomposite driven by visible light. Chem Eng J [Internet] 2018;350:1043–55. Available from: http://www.sciencedirect.com/science/article/pii/S1385894718310842
18. Nguyen TB, Huang CP, Doong R An. Photocatalytic degradation of bisphenol a over a ZnFe 2 O 4 /TiO 2 nanocomposite under visible light. Sci. Total environ. [internet] 2019;646:745–56. Available from: https://doi.org/10.1016/j.scitotenv.2018.07.352, 2019.
19. Aghamali A, Khosravi M, Hamishehkar H, Modirshahla N, Behnajady MA. Preparation of novel high performance recoverable and natural sunlight-driven nanocomposite photocatalyst of Fe3O4/C/TiO2/N-CQDs. Mater. Sci. Semicond. Process. [internet] 2018;87:142–54. Available from: https://doi.org/10.1016/j.mssp.2018.07.018, 2018.
20. Jafari AJ, Mahrooghi M, Moslemzadeh M. Removal of Escherichia coli from synthetic turbid water using titanium tetrachloride and zirconium tetrachloride as coagulants. Desalin Water Treat. 2019;163:358–65.

21. Gu Y, Yperman J, Carleer R, D'Haen J, Maggen J, Vanderheyden S, et al. Adsorption and photocatalytic removal of ibuprofen by activated carbon impregnated with TiO2 by UV–Vis monitoring. Chemosphere [internet] 2019;217:724–31. Available from: https://doi.org/10.1016/j.chemosphere.2018.11.068, 2019.
22. Xue G, Liu H, Chen Q, Hills C, Tyrer M, Innocent F. Synergy between surface adsorption and photocatalysis during degradation of humic acid on TiO2/activated carbon composites. J. Hazard. Mater. [internet] 2011;186:765–72. Available from: https://doi.org/10.1016/j.jhazmat.2010.11.063, 2011.
23. Law M, Greene LE, Johnson JC, Saykally R, Yang P. Nanowire dye-sensitized solar cells. Mater Sustain Energy A Collect Peer-Reviewed Res Rev Artic from Nat Publ Gr. 2010;4:75–9.
24. Xu X, Liu R, Cui Y, Liang X, Lei C, Meng S, et al. PANI/FeUiO-66 nanohybrids with enhanced visible-light promoted photocatalytic activity for the selectively aerobic oxidation of aromatic alcohols. Appl. Catal. B environ. [internet] 2017;210:484–94. Available from: https://doi.org/10.1016/j.apcatb.2017.04.021, 2017.
25. Benyamina I, Manseri K, Mansour M, Benalioua B, Bentouami A, Boury B. New bi 2 O 3 -ZnO composite deposited on glass wool. Effect of the synthesis method on photocatalytic efficiency under visible light. Appl. Surf. Sci. [internet] 2019;483:859–69. Available from: https://doi.org/10.1016/j.apsusc.2019.03.310, 2019.
26. Nishimura A, Zhao X, Hayakawa T, Ishida N, Hirota M, Hu E. Impact of overlapping Fe/TiO2 prepared by sol-gel and dip-coating process on CO2 reduction. Int. J. Photoenergy 2016;2016.
27. Tian L, Xing L, Shen X, Li Q, Ge S, Liu B, et al. Visible light enhanced Fe–I–TiO2 photocatalysts for the degradation of gaseous benzene. Atmos. Pollut. Res. [Internet] 2020;11:179–85. Available from: http://www.sciencedirect.com/science/article/pii/S1309104219304799
28. Chen Q, Chen L, Qi J, Tong Y, Lv Y, Xu C, et al. Photocatalytic degradation of amoxicillin by carbon quantum dots modified K2Ti6O13 nanotubes: Effect of light wavelength. Chinese Chem. Lett. [Internet] 2019;Available from: https://doi.org/10.1016/j.cclet.2019.03.002
29. Gu L, Chen Z, Sun C, Wei B, Yu X. Photocatalytic degradation of 2, 4-dichlorophenol using granular activated carbon supported TiO2. Desalination. 2010;263:107–12.
30. Lee JC, Kim MS, Kim BW. Removal of paraquat dissolved in a photoreactor with TiO2 immobilized on the glass-tubes of UV lamps. Water Res. 2002;36:1776–82.
31. Dehghani MH, Kamalian S, Shayeghi M, Yousefi M, Heidarinejad Z, Agarwal S, et al. High-performance removal of diazinon pesticide from water using multi-walled carbon nanotubes. Microchem. J. [internet] 2019;145:486–91. Available from: https://doi.org/10.1016/j.microc.2018.10.053, 2019.
32. Kaur T, Sraw A, Wanchoo RK, Toor AP. Solar assisted degradation of carbendazim in water using clay beads immobilized with TiO2 & Fe doped TiO2. Sol. Energy [internet] 2018;162:45–56. Available from: https://doi.org/10.1016/j.solener.2017.11.033, 2018.
33. Lin S, Zhang X, Sun Q, Zhou T, Lu J. Fabrication of solar light induced Fe-TiO2 immobilized on glass-fiber and application for phenol photocatalytic degradation. Mater. Res. Bull. [internet] 2013;48:4570–5. Available from: https://doi.org/10.1016/j.materresbull.2013.07.063, 2013.
34. Wang CY, Böttcher C, Bahnemann DW, Dohrmann JK. A comparative study of nanometer sized Fe(III)-doped TiO2 photocatalysts: synthesis, characterization and activity. J Mater Chem. 2003;13:2322–9.
35. Chen P, Wang F, Chen ZF, Zhang Q, Su Y, Shen L, et al. Study on the photocatalytic mechanism and detoxicity of gemfibrozil by a sunlight-driven TiO2/carbon dots photocatalyst: the significant roles of reactive oxygen species. Appl. Catal. B environ. [internet] 2017;204:250–9. Available from: https://doi.org/10.1016/j.apcatb.2016.11.040, 2017.
36. Jafari AJ, Moslemzadeh M. Synthesis of Fe-doped TiO 2 for Photocatalytic processes under UV-visible light : effect of preparation methods on crystal size — a systematic review study. COMMENTSONINORGANIC Chem 2020;
37. Taghavi K, Naghipour D, Mohagheghian A, Moslemzadeh M, Taghavi K, Moslemzadeh M, et al. Adsorption of chromium(VI) from aqueous solution by Artist's bracket fungi. Water Sci. Technol. [internet] 2017;158:207–15. Available from: https://doi.org/10.1080/01496395.2017.1299179, 2017.
38. Pourkarim S, Ostovar F, Mahdavianpour M, Moslemzadeh M. Adsorption of chromium(VI) from aqueous solution by Artist's bracket fungi. Sep. Sci. Technol. [internet] 2017;52:1733–41. Available from: https://doi.org/10.1080/01496395.2017.1299179, 2017.
39. Ibrahim SA, Anwar MK, Ainuddin AR, Hariri A, Rus AZM, Kamdi Z, et al. Synthesis and characterization of visible light active Fe-TiO2 using hydrothermal method. Int J Integr Eng [Internet] 2019;11:80–5. Available from: https://www.scopus.com/inward/record.uri?eid=2-s2.0-85074842080&doi=10.30880%2Fijie.2019.11.05.011&partnerID=40&md5=cfce9a4ca5be1bc632af2cc125fc748b
40. Esrafili A, Bagheri S, Kermani M, Gholami M, Moslemzadeh M. Simultaneous adsorption of heavy metal ions (Cu2+ and Cd2+) from aqueous solutions by magnetic silica nanoparticles (Fe3O4@SiO2) modified using edta. Desalin Water Treat. 2019;158:207–15.
41. Li K, Wang H, Pan C, Wei J, Xiong R, Shi J. Enhanced photoactivity of Fe + N Codoped anatase-rutile TiO 2 nanowire film under visible light irradiation. Int J Photoenergy. 2012;2012:1–8.
42. Arias LMF, Duran AA, Cardona D, Camps E, Gómez ME, Zambrano G. Effect of annealing treatment on the photocatalytic activity of TiO2 thin films deposited by dc reactive magnetron sputtering. J Phys Conf Ser. 2015;614:012008.
43. Yadav HM, Kolekar TV, Pawar SH, Kim J-S. Enhanced photocatalytic inactivation of bacteria on Fe-containing TiO2 nanoparticles under fluorescent light. J Mater Sci Mater Med. 2016;27:57.
44. Aghamali A, Khosravi M, Hamishehkar H, Modirshahla N, Behnajady MA. Preparation of novel high performance recoverable and natural sunlight-driven nanocomposite photocatalyst of Fe3O4/C/TiO2/N-CQDs. Mater Sci Semicond Process [Internet] 2018;87:142–54. Available from: http://www.sciencedirect.com/science/article/pii/S136980011732560X
45. Jafari AJ, Moslemzadeh M. Synthesis of Fe-doped TiO 2 for Photocatalytic processes under UV-visible light : effect of preparation methods on crystal size — a systematic review study. Commentsoninorganic Chem. [internet] 2020;00:1–20. Available from: https://doi.org/10.1080/02603594.2020.1821674, 2020.
46. Zhang J, Kuang M, Wang J, Liu R, Xie S, Ji Z. Fabrication of carbon quantum dots/TiO2/Fe2O3 composites and enhancement of photocatalytic activity under visible light. Chem. Phys. Lett. [internet] 2019;730:391–8. Available from: https://doi.org/10.1016/j.cplett.2019.06.011, 2019.
47. Jonidi A, Moslemzadeh M. Adsorption of lead (Pb 2 +) onto salicylic acid-methanol modified steel slag from aqueous solution : a cost analysis. 2020;198:200–10.
48. Zhao X, Du P, Cai Z, Wang T, Fu J, Liu W. Photocatalysis of bisphenol a by an easy-settling titania/titanate composite: effects of water chemistry factors, degradation pathway and theoretical calculation. Environ Pollut [Internet] 2018;232:580–90. Available from: http://www.sciencedirect.com/science/article/pii/S0269749117313799
49. Ahamad T, Naushad M, Ruksana, Alhabarah AN, Alshehri SM. N/S doped highly porous magnetic carbon aerogel derived from sugarcane bagasse cellulose for the removal of bisphenol-a. Int. J. Biol.

Macromol. [internet] 2019;132:1031–8. Available from: https://doi.org/10.1016/j.ijbiomac.2019.04.004, 2019.
50. Frontistis Z, Daskalaki VM, Katsaounis A, Poulios I, Mantzavinos D. Electrochemical enhancement of solar photocatalysis: degradation of endocrine disruptor bisphenol-a on Ti/TiO2 films. Water Res [Internet] 2011;45:2996–3004. Available from: http://www.sciencedirect.com/science/article/pii/S0043135411001412
51. Yari K, Seidmohammadi A, Khazaei M, Bhatnagar A, Leili M. A comparative study for the removal of imidacloprid insecticide from water by chemical-less UVC, UVC/TiO2 and UVC/ZnO processes. J Environ Heal Sci Eng. 2019;17:337–51.
52. Zhou G, Cao Y, Jin Y, Wang C, Wang Y, Hua C, et al. Novel selective adsorption and photodegradation of BPA by molecularly imprinted sulfur doped nano-titanium dioxide. J. Clean. Prod. [internet] 2020;274:122929. Available from: https://doi.org/10.1016/j.jclepro.2020.122929, 2020.
53. Armaković SJ, Grujić-Brojčin M, Šćepanović M, Armaković S, Golubović A, Babić B, et al. Efficiency of La-doped TiO2 calcined at different temperatures in photocatalytic degradation of β-blockers. Arab J Chem. 2019;12:5355–69.
54. Mahdavianpour M, Ildari S, Ebrahimi M, Moslemzadeh M. Decolorization and Mineralization of Methylene Blue in Aqueous Solutions by Persulfate / Fe 2 + Process. 2020;42:244–51.
55. Kujlu R, Moslemzadeh M, Rahimi S, Aghayani E, Ghanbari F, Mahdavianpour M. Selecting the best stabilization/solidification method for the treatment of oil-contaminated soils using simple and applied best-worst multi-criteria decision-making method. Environ. Pollut. [internet] 2020;263:114447. Available from: https://doi.org/10.1016/j.envpol.2020.114447, 2020.
56. Liu CM, Diao ZH, Huo WY, Kong LJ, Du JJ. Simultaneous removal of Cu2+ and bisphenol a by a novel biochar-supported zero valent iron from aqueous solution: synthesis, reactivity and mechanism. Environ. Pollut. [internet] 2018;239:698–705. Available from: https://doi.org/10.1016/j.envpol.2018.04.084, 2018.
57. Jaseela PK, Shamsheera KO, Joseph A. Mesoporous Titania-silica nanocomposite as an effective material for the degradation of Bisphenol a under visible light. J Saudi Chem Soc. 2020;24:651–62.
58. Taghavi K, Naghipour D, Mohagheghian A, Moslemzadeh M. Photochemical degradation of 2,4-dichlorophenol in aqueous solutions by Fe2+/ Peroxydisulfate/ UV process. Int J Eng [Internet] 2017;30:15–22. Available from: http://www.ije.ir/Vol30/No1/A/3.pdf